

Research Report: Regular Manuscript

Distinct oscillatory dynamics underlie different components of hierarchical cognitive control

<https://doi.org/10.1523/JNEUROSCI.0617-20.2020>

Cite as: J. Neurosci 2020; 10.1523/JNEUROSCI.0617-20.2020

Received: 16 March 2020

Revised: 11 May 2020

Accepted: 12 May 2020

This Early Release article has been peer-reviewed and accepted, but has not been through the composition and copyediting processes. The final version may differ slightly in style or formatting and will contain links to any extended data.

Alerts: Sign up at www.jneurosci.org/alerts to receive customized email alerts when the fully formatted version of this article is published.

1 **Title**

2 Distinct oscillatory dynamics underlie different components of hierarchical cognitive control

3 **Authors**

4 Justin Riddle^{1,2,3,7}, David A. Vogelsang^{1,4}, Kai Hwang^{4,5}, Dillan Cellier^{5,6}, Mark
5 D'Esposito^{2,4}

6 **Affiliations**

- 7 1. These authors contributed equally
8 2. Department of Psychology, University of California, Berkeley, 2121 Berkeley Way,
9 Berkeley, CA 94720-1650
10 3. Department of Psychiatry, University of North Carolina at Chapel Hill, 101 Manning
11 Drive, Chapel Hill, NC 27514
12 4. Helen Wills Neuroscience Institute, University of California, Berkeley, 450 Li Ka
13 Shing Biomedical Center, MC#3370, Berkeley, CA 94720-3370
14 5. Department of Psychology, University of Iowa, 301 E Jefferson Street, Iowa City, IA,
15 52245
16 6. Department of Cognitive Science, University of California, Berkeley, 140 Stephens
17 Hall, Berkeley, CA 94720-2306
18 7. Corresponding author

19 **Corresponding author**

20 Justin Riddle
21 riddler@berkeley.edu
22 210 Barker Hall
23 Berkeley, CA, 94720

24 **Number of pages:** 30

25 **Number of figures:** 8

26 **Number of words:** Abstract – 225; Introduction – 517; Discussion – 1511

27 **Conflicts of Interest**

28 The authors declare no competing financial interests.

29 **Acknowledgements**

30 J.R., D.V., K.H., and M.D. designed the research. J.R., D.V., K.H. and D.C. performed
31 experiments. J.R., D.V., and K.H. analyzed the data. J.R., D.V., K.H., and M.D. wrote the
32 manuscript. This work was supported by National Institutes of Health grants R01 MH111737

33 and R01 MH063901 awarded to M.D. and National Science Foundation grant DGE 1106400
34 awarded to J.R.

35 **Abstract**

36

37 Hierarchical cognitive control enables us to execute actions guided by abstract goals. Previous
38 research has suggested that neuronal oscillations at different frequency bands are associated
39 with top-down cognitive control, however, whether distinct neural oscillations have similar or
40 different functions for cognitive control is not well understood. The aim of the current study was
41 to investigate the oscillatory neuronal mechanisms underlying two distinct components of
42 hierarchical cognitive control: the level of abstraction of a rule, and the number of rules that
43 must be maintained (set-size). We collected electroencephalography (EEG) data in 31 men and
44 women who performed a hierarchical cognitive control task that varied in levels of abstraction
45 and set-size. Results from time-frequency analysis in frontal electrodes showed an increase in
46 theta amplitude for increased set-size, whereas an increase in delta was associated with
47 increased abstraction. Both theta and delta amplitude correlated with behavioral performance in
48 the tasks but in an opposite manner: theta correlated with response time slowing when the
49 number of rules increased whereas delta correlated with response time when rules became
50 more abstract. Phase amplitude coupling analysis revealed that delta phase coupled with beta
51 amplitude during conditions with a higher level of abstraction, whereby beta band may
52 potentially represent motor output that was guided by the delta phase. These results suggest
53 that distinct neural oscillatory mechanisms underlie different components of hierarchical
54 cognitive control.

55 **Significance Statement**

56

57 Cognitive control allows us to perform immediate actions while maintaining more abstract,
58 overarching goals in mind and to choose between competing actions. We found distinct
59 oscillatory signatures that correspond to two different components of hierarchical control: the
60 level of abstraction of a rule and the number of rules in competition. An increase in the level of
61 abstraction was associated with delta oscillations, whereas theta oscillations were observed
62 when the number of rules increased. Oscillatory amplitude correlated with behavioral
63 performance in the task. Finally, the expression of beta amplitude was coordinated via the
64 phase of delta oscillations, and theta phase coupled with gamma amplitude. These results
65 suggest that distinct neural oscillatory mechanisms underlie different components of hierarchical
66 cognitive control.

67 **Introduction**

68

69 Cognitive control orchestrates thoughts and actions according to internal goals (Norman and
70 Shallice 1986, Braver 2012). The frontal cortex is central to cognitive control, where
71 representations of rules and goals provide top-down influences over motor and perceptual
72 systems to guide actions (Miller and Cohen 2001, Miller and D'Esposito 2005, Badre and Nee
73 2018, Vogelsang and D'Esposito 2018). Previous research findings suggest that the frontal
74 cortex is organized hierarchically along the rostral-caudal axis, where the caudal frontal cortex is
75 involved in the control of concrete action representations, whereas the rostral prefrontal cortex
76 is involved in the control of abstract rules, goals, and contexts (Badre and Nee 2018). We have
77 previously demonstrated that at any particular level of representation, an appropriate action can
78 be chosen from a number of competing rules (number of rules defined as set-size), and as
79 competition increases, cognitive control is required to adjudicate among alternatives (Badre and
80 D'Esposito 2007).

81 It is proposed that rhythmic neural oscillations support a diverse range of cognitive
82 functions, whereby oscillations in different frequency bands, ranging from slow delta oscillations
83 to faster gamma oscillations, are generated by distinct biophysical mechanisms and are
84 associated with different cognitive functions (for reviews see: (Sauseng, Griesmayr et al. 2010,
85 Roux and Uhlhaas 2014, Helfrich and Knight 2016, Sadaghiani and Kleinschmidt 2016, Helfrich,
86 Breska et al. 2019)). Phase amplitude coupling (PAC) between frequency bands, in which the
87 phase of a slow oscillation like theta can modulate the amplitude of faster oscillations like
88 gamma (Lisman and Jensen 2013, Nácher, Ledberg et al. 2013, Arnal, Doelling et al. 2014,
89 Morillas-Romero, Tortella-Feliu et al. 2015, Voytek, Kayser et al. 2015, Heusser, Poeppel et al.
90 2016), further supports inter-areal communication and interactions between cognitive functions.
91 However, whether or not there are distinct neural oscillations associated with different
92 components of hierarchical cognitive control is unknown.

93 In our previous human electrocorticography (ECoG) study, we found that tasks that
94 required increased hierarchical cognitive control were associated with increased theta-band
95 synchronization between the prefrontal and premotor/motor regions (Voytek, Kayser et al.
96 2015). Furthermore, the phase of prefrontal theta oscillations showed increased coupling with
97 the amplitude of gamma oscillations in the motor cortex (Voytek, Kayser et al. 2015). A series of
98 non-human primate experiments have also found that beta-band oscillations are associated with
99 rule representation in the frontal cortex, in which distinct neural populations represent different
100 rules, and become more synchronized in beta frequency when the rule is behaviorally relevant
101 (Buschman, Denovellis et al. 2012, Antzoulatos and Miller 2014, Antzoulatos and Miller 2016,
102 Wutz, Loonis et al. 2018). Furthermore, updating the active rule representation increases delta
103 oscillations in these same neural populations, preceded by a modulation in beta oscillations
104 (Antzoulatos and Miller 2016). Together, these findings suggest that theta-gamma and delta-
105 beta band oscillations are associated with hierarchical cognitive control. However, in these
106 experiments, tasks that engaged more abstract rules also had higher set-size (higher number of
107 rules to select from), making it impossible to determine if the modulation of neural oscillations
108 and phase-amplitude coupling by these cognitive processes are driven by set size or
109 abstraction. In this study, our aim was to address this question.

110

111 **Materials and Methods**

112

113 *Experimental Design and Statistical Analysis*

114 Thirty-one healthy participants (18 females; mean age = 20 years; range 18-34) with
115 normal or corrected to normal vision were recruited from the University of California, Berkeley.
116 Written consent was obtained prior to the start of the experiment and participants received
117 monetary compensation for their participation. The study was approved by the University of
118 California, Berkeley Committee for Protection of Human Subjects.

119 The experiment consisted of a single session of EEG during performance of the
120 hierarchical cognitive control task. Behavioral performance, response time and accuracy, was
121 analyzed using two-way repeated-measures ANOVA with two factors: abstraction (high and low)
122 and set-size (high and low). Time frequency analysis was conducted using stimulus and
123 response-locked epochs for the abstraction and set-size contrast. The time frequency analysis
124 was restricted to a midfrontal electrode cluster that was defined using hierarchical clustering of
125 the time frequency data independent of the contrasts of interest. We corrected for multiple
126 comparisons and spurious findings using permutation testing with significance determined by
127 cluster mass across all seven electrode clusters for the abstraction and set-size contrast. Next,
128 the significant time frequency bands were correlated with response time as a function of
129 abstraction and set-size using Pearson correlation. Finally, phase amplitude coupling (PAC)
130 was computed between delta phase and beta amplitude and theta phase and gamma amplitude
131 for each task condition. PAC values were inputted to a two-way repeated-measures ANOVA
132 with two factors: abstraction and set-size.

133

134 *Experimental Task*

135 The task used in this study was adapted from two previously published studies (Badre
136 and D'Esposito 2007, Badre and D'Esposito 2009, Voytek, Kayser et al. 2015). We manipulated
137 two components of hierarchical cognitive control, abstraction and set-size (see Figure 1A).
138 During the response task (low abstraction conditions), participants learned the association
139 between a colored square and a button response. The response task had two levels of set-size:
140 a low set-size condition (in which four colored squares had to be associated with four
141 responses) and a high set-size condition (in which eight different colored squares had to be
142 associated with eight response options; Figure 1A). In the dimension task (high abstract
143 conditions), participants were presented with a colored square that contained two objects. The
144 color of the square indicated the dimension (shape or texture) by which the participant had to

145 evaluate the two objects. Importantly, the abstraction task contained two levels of set-size
146 similar to the response task: a low level of set-size and yet still higher in abstraction and a
147 higher level of set-size and also high in abstraction (see Figure 1A). In the high abstraction, low
148 set-size condition, participants made a judgement along only one dimension (either shape or
149 texture) as both colored squares mapped to a single dimension (e.g. a purple square or a green
150 square signal that participants must judge whether the two objects have the same or different
151 shape). In the high abstraction, high set-size condition, two colored squares mapped to two
152 different dimensions (e.g. the color red indicates a perceptual judgement along the shape
153 dimension, the color blue indicates the texture dimension).

154 Our previous versions of the experiment (Badre and D'Esposito 2007, Voytek, Kayser et
155 al. 2015) did not match performance between the low and high abstraction tasks, as the highest
156 set-size condition of a low abstraction task showed worse performance than the lowest set-size
157 of a high abstraction task. By matching performance across levels of abstraction, we remove a
158 potential confound of task difficulty in isolating the processing of abstract rule representations
159 (Todd, Nystrom et al. 2013). To match performance between levels of abstraction, we ran
160 multiple pilot experiments, in which we increased the difficulty of the response task into a
161 comparable performance range as the dimensions task. In particular, we iteratively increased
162 the number of competing rules in the response task and shorted the response window from
163 three to two seconds to increase response time and reduce the accuracy of participants for the
164 response task. At the completion of this pilot testing, we selected two conditions to be defined
165 as low set-size based on performance levels: the response task with four responses and the
166 dimensions task with one dimension. For the high set-size conditions, we used the response
167 task with eight responses and the dimension task with two dimensions.

168 In the experiment, participants performed eight blocks, two of each of the four
169 conditions. Each block contained 48 trials; thus, each participant completed 96 trials per
170 experimental condition. Each trial was presented on the screen for two seconds and participants

171 were instructed to provide their response within that time window. Each trial was separated by a
172 fixation cross that varied exponentially in length from three to ten seconds. The experiment was
173 programmed in Psychtoolbox implemented in MatLab 2015a (The MathWorks, Inc.). Prior to the
174 start of the experimental task, participants were instructed to maintain their gaze on a fixation
175 point and to remain still for five minutes with eyes open followed by five minutes eyes closed.
176 This resting-state EEG data was not analyzed for the purpose of this paper.

177

178 *EEG Recording and Preprocessing*

179 EEG data was recorded from 64 active electrodes using a BioSemi ActiveTwo amplifier
180 with Ag-AgCl pin-type active electrodes mounted on an elastic cap according to the extended
181 10-20 system (BioSemi, Amsterdam, Netherlands). In addition, four electrodes were used to
182 monitor horizontal and vertical eye movements and two electrodes recorded electrical activity
183 from the mastoids. Signals were amplified and digitized at 1,024 Hz and stored for offline
184 analysis. Participants were trained before the experiment to minimize eye movements, blinking,
185 and muscle movement before the experiment.

186 The EEG data were analyzed with the software package EEGLab14 (Delorme and
187 Makeig, 2004) which utilized MatLab2015a (The MathWorks, Inc.). The continuous EEG data
188 were re-referenced to an average of the mastoid electrodes and filtered digitally with a
189 bandpass of 0.1-100Hz (two-way least-squares finite impulse response filter). The continuous
190 data were then divided into epochs ranging from -1000 milliseconds before stimulus onset until
191 2000 milliseconds post-stimulus onset. The epochs in the EEG data were visually inspected and
192 trials that contained excessive noise, such as muscle artifacts, were removed, resulting in an
193 average of 4.5% of trials that were removed across participants. Furthermore, electrode
194 channels with excessive noise were identified by visual inspection and reconstructed using the
195 average of neighboring electrodes. Eye-blinks and other EEG related artifacts were identified

196 and rejected using the extended info-max independent component analysis using the EEGLab
197 toolbox with default mode training parameters (Delorme and Makeig 2004).

198

199 *Electrode clustering*

200 Electrode clusters were defined based on a data-driven hierarchical clustering approach
201 that grouped electrodes based on the similarity of the evoked oscillatory amplitude that ranged
202 from 2-30Hz (see for similar procedure (Clarke, Roberts et al. 2018). Time-frequency
203 decomposition was averaged across all trials, conditions, and participants. Data from each
204 electrode was vectorized such that it included all time points and frequencies. A distance metric
205 was calculated for each electrode based on the similarity in evoked spectral response. An
206 agglomerative hierarchical clustering algorithm was applied that grouped pairs of electrodes
207 with the most similar spectral response. The two most similar electrode pairs were averaged.
208 This process continued until all electrodes were paired under a single tree. A dendrogram of the
209 hierarchical clusters was created and only clusters that fit an a priori cluster scheme based on
210 Clarke et al. (2018) were included in the time-frequency analysis. Each electrode cluster was
211 defined to only include contiguous electrodes and we excluded electrode clusters with less
212 than three electrodes. This hierarchical clustering approach resulted in six electrode clusters
213 that were used in the main analysis (Figure 2). Results reported here for an electrode cluster is
214 the averaged spectral response of all electrodes within the cluster. Our previous evidence using
215 this task in fMRI (Badre and D'Esposito 2007) and electrocorticography (Voytek, Kayser et al.
216 2015) found task-modulated activity related to cognitive control in lateral prefrontal cortex.
217 However, due to the problem of volume conduction and electric field properties in EEG,
218 activation of bilateral sites is commonly found in the midline (Sasaki, Tsujimoto et al. 1996,
219 Stropahl, Bauer et al. 2018, Riddle, Ahn et al. 2020). Therefore, we focused our analysis on the
220 frontal midline electrode cluster and capitalized on the temporal resolution afforded by EEG. We

221 hypothesized that the frontal midline electrode clusters (highlighted in Figure 2) would show the
222 strongest effects of hierarchical cognitive control (see (Cavanagh and Frank 2014) for review).

223

224 *Time-frequency Analysis*

225 Time-frequency analysis was applied using six cycle Morlet wavelet in the frequency
226 range of 2 to 50 Hz with steps of 1 Hz between each wavelet center. The Morlet wavelets were
227 applied to sliding time windows of 20 milliseconds increments in the entire epoch ranging from -
228 1000 milliseconds to 2000 milliseconds with stimulus onset set as time 0. To minimize the
229 problem of edge artifacts, we concatenated mirrored (i.e. time inverted) segments before and
230 after the task epoch (Cohen 2014). Time-frequency analysis was performed on these extended
231 epochs and mirrored segments were discarded from the final analysis (see for similar procedure
232 (Fell and Axmacher 2011, Vogelsang, Gruber et al. 2018)). Results reported here were not
233 baseline corrected since we were interested in differences across conditions and therefore
234 baseline correction is not necessary (see for similar approaches (Fell and Axmacher 2011,
235 Gruber, Watrous et al. 2013, Vogelsang, Gruber et al. 2018)). For each of the four experimental
236 conditions, only trials in which the participant made a correct response were included in the
237 analysis. Trial numbers used in the analysis were: low abstraction, low set-size mean(std) =
238 92.4(4.8), range 76 - 96; low abstraction, high set-size mean(std) = 88.1(8.0), range 56-96; high
239 abstraction, low set-size mean(std) = 91.8(6.8), range 68-96; high abstraction, high set-size
240 mean(std) = 87.1(7.4), range 68-96. Our main analysis was two contrasts, one for “abstraction”
241 (high versus low) and one for “set-size” (high versus low).

242 An across participant non-parametric statistical approach was applied to test for
243 significant time-frequency differences between the contrasts of interest. We ran cluster-mass
244 permutation testing in which the average t-value within a significant cluster ($p < 0.05$) is used to
245 evaluate significance. The permutation testing procedure consisted of the following steps. First,
246 we computed the cluster mass for each of the contrasts of interest (abstraction and set-size) for

247 each of the six electrode clusters. Second, the experimental conditions for the abstraction (or
248 set-size) contrast were randomly swapped for 50% of the participants such that any systematic
249 differences between the conditions were eliminated. We ran the contrast for this randomized
250 pairing and calculated the largest absolute cluster mass across all electrode clusters. This
251 randomization process was repeated 1000 times to create a null distribution of the largest
252 negative and positive cluster mass values. Using an alpha level of .05 with 1000 permutations,
253 we used the 25th and 975th values to represent the critical mass values, and values below or
254 higher than these values were considered to be significant effects. This stringent procedure
255 allowed us to control for multiple comparisons across the electrode clusters (Blair and Karniski
256 1993, Maris and Oostenveld 2007).

257

258 *Phase Amplitude Coupling Analysis*

259 In addition to a time-frequency analysis, we also sought evidence for how different
260 frequency bands may interact with each other during hierarchical cognitive control. One possible
261 mechanism is phase amplitude coupling (PAC), which involves examining the relationship
262 between the phase of a lower frequency band (e.g. delta and theta) and the amplitude of a
263 higher frequency band (e.g. beta and gamma). To examine whether the phase of slow
264 oscillatory bands modulated the amplitude of faster frequency bands as a function of increased
265 rule abstraction and rule set-size, we computed PAC for the phase of slow frequency bands in
266 the range of 2-7 Hz, which includes delta and theta, with the amplitude of the higher frequency
267 spectrum ranging from 10-49 Hz separately for each task condition. We narrowed our analysis
268 to the coupled pairs motivated by our time-frequency analysis and a priori based on our
269 previous findings (Voytek, Kayser et al. 2015).

270 To compute PAC, we extracted the phase of the delta and theta frequency bands using
271 a three cycle Morlet wavelet convolution and the amplitude of the higher frequencies using a
272 five cycle Morlet wavelet convolution. We selected these parameters such that the half width full

273 mass of the low and high frequencies were more closely matched (Cohen 2019). We calculated
274 PAC using the phase and amplitude values from the significant time windows observed in the
275 time-frequency contrast for delta band (200 to 1400 milliseconds) and theta band (600 to 1200
276 milliseconds). For each participant, the phase (θ) and amplitude (M) values of each trial were
277 concatenated into a single continuous time series (n is the number of time points) and PAC was
278 calculated according to **Formula 1**.

279 **Formula 1.**
$$PAC = \left| \frac{\sum_{t=1}^n M * e^{i\theta}}{n} \right|$$

280 We applied nonparametric permutation testing to determine whether the obtained PAC
281 values would be expected given the null hypothesis of no relationship between phase and
282 amplitude. The permutation procedure involved temporally shifting the amplitude values with a
283 random temporal offset of at least 10% the length of the time series and calculating PAC
284 (Cohen 2014). After 1000 repetitions, PAC is converted into a z-score from the null distribution,
285 resulting in PAC_z. We were interested in changes in PAC_z with increased abstraction and set-
286 size. In order to reduce multiple comparisons, we used a priori coupled pairs for the
287 hypothesized coupled frequencies based on the time-frequency analysis and ran a two-way
288 repeated-measures ANOVA of within-participant factors: abstraction and set-size.

289

290 *Code and Data Availability*

291 Custom code used for these analyses are available upon request to the corresponding
292 author. The authors assert that all requests for raw data within reason will be fulfilled by the
293 corresponding author.

294

295 **Results**

296

297 *Behavioral Results*

298 The task was designed to separately manipulate abstraction and set size during
299 hierarchical cognitive control. To test the effects of our behavioral manipulation, we performed
300 separate two-way repeated-measures ANOVA. We entered two independent variables:
301 abstraction (low, high) and set-size (low, high), and response time (RT) and accuracy as
302 dependent variables. For RT, the ANOVA revealed a significant main effect of abstraction (high
303 abstraction mean = 1132.0, sd = 105.3 milliseconds; low abstraction mean = 974.1, sd = 95.0
304 milliseconds; $F(1,30) = 398$, $p < 0.0001$, $\eta_p^2 = 0.93$), a main effect of set-size (high set-size mean
305 = 1176.0, sd = 95.7 milliseconds; low set-size mean = 930.1, sd = 95.5 milliseconds; $F(1,30) =$
306 92.1 , $p < 0.0001$, $\eta_p^2 = 0.75$), and an interaction ($F(1,30) = 53.1$, $p < 0.0001$, $\eta_p^2 = 0.64$) (Figure
307 1B). Participants were slower as a function of abstraction and set-size. For accuracy, the
308 ANOVA revealed a main effect of set-size (high set-size mean = 94.7%, sd = 5.0%; low set-size
309 mean = 97.7%, sd = 2.9%; $F(1,30) = 10.2$, $p = 0.003$, $\eta_p^2 = 0.25$), but did not reveal a significant
310 main effect of abstraction ($F(1,30) = 0.11$, $p = 0.75$, $\eta_p^2 = 0.0036$) or interaction (Figure 1C).
311 Participants were less accurate for the conditions that required maintenance of a larger set-size,
312 but behavior was matched across levels of abstraction.

313

314 *Time-Frequency Results*

315 We performed time-frequency analyses to determine how set-size and abstraction
316 modulates patterns of neural oscillations during hierarchical cognitive control. The time-
317 frequency analyses focused on the spectral amplitude differences ranging from 2 to 50 Hz in the
318 entire epoch time window (-1000 to 2000 milliseconds relative to stimulus onset) for both the
319 abstraction and set-size contrast (high versus low abstraction and high versus low set size). For
320 the abstraction contrast (Figure 3A), across all electrode clusters, there was a significant
321 increase in the delta frequency band (2-3 Hz) from 100 to 2000 milliseconds post stimulus onset
322 and a significant decrease in the beta frequency band (peak at 12-22 Hz) from 500 to 1500
323 milliseconds post stimulus onset (peak at 500 to 1000 milliseconds) for all electrode clusters. In

324 the topographic plots, it can be seen that in the abstraction contrast, delta amplitude showed the
325 strongest increase in mid and right frontal electrode clusters (Figure 3B) whereas beta
326 amplitude showed the strongest decrease in the mid frontal electrode cluster (Figure 3C). For
327 the set-size contrast (Figure 3D), across all electrode clusters, there was a significant increase
328 in amplitude in the theta frequency band (4-6 Hz) from 850 to 1700 milliseconds post stimulus
329 onset. There was a significant decrease in amplitude in the beta frequency band (12-30 Hz)
330 around 500 to 1500 milliseconds after stimulus onset in frontal midline electrode cluster, and
331 500 to 1800 milliseconds after stimulus onset in central and posterior electrode clusters. In the
332 topographic plots, it can be seen that in the set-size contrast, theta amplitude showed the
333 strongest increase in the frontal midline electrode cluster and beta amplitude showed the
334 strongest decrease in the frontal midline and central midline electrode clusters. Altogether, two
335 different low frequency bands increased in amplitude in the midfrontal electrode cluster. Delta
336 amplitude increased for abstraction and theta amplitude increased for set-size. However, beta-
337 band amplitude decreased for both higher abstraction and higher set size, but with a slightly
338 different spread in frequency within the beta-band. Peak beta amplitude modulation for the
339 abstraction contrast occupied a lower frequency range, from 12-18 Hz, compared to the wider
340 frequency range in peak beta amplitude modulation for the set-size contrast from 12-22 Hz.

341 In order to better understand the timecourse of amplitude modulations found for the
342 contrasts of interest, the time course for the amplitude of delta, theta and beta frequency bands
343 in the frontal midline cluster is plotted in Figure 4. Approximately 500 milliseconds after stimulus
344 onset, the high abstraction, high set-size condition showed the greatest delta amplitude
345 increase followed by high abstraction, low set-size and then both low abstraction conditions
346 (Figure 4A). Approximately 1200 to 1800 milliseconds after stimulus onset, the two high set-size
347 conditions showed an increase in theta amplitude (Figure 4B). Thus, both delta and theta
348 frequency bands showed increased amplitude sustained throughout stimulus processing for
349 greater abstraction or set-size. Finally, there was a decrease in amplitude in the beta frequency

350 band for all four conditions for the first 600 milliseconds (Figure 4C). However, only the high
351 abstraction, high set-size condition showed a significant and prolonged decrease in beta
352 amplitude relative to the other three conditions from 600 to 1600 milliseconds after stimulus
353 onset.

354 Since the stimulus-locked time-frequency effects persist after the probe for over a
355 second, it is possible that decreased beta amplitude was related to a systematic difference in
356 response time between conditions, and low-frequency activity in delta and theta band might only
357 be significantly elevated after a response is made reflecting post-response monitoring
358 processes. If decreased beta amplitude was indeed driven by motor-related processes, then it
359 would not be observed in a response-locked analysis. If low frequency activity reflects post-
360 response monitoring processes, then it would only be observed after the response in a
361 response-locked analysis. We performed a response-locked time-frequency analysis on the
362 abstraction and set-size contrast in the midfrontal electrode cluster (Figure 5). For the
363 abstraction contrast (Figure 5A), there was a significant decrease in amplitude in the beta
364 frequency band (10-20 Hz) just prior to a response, whereas there was no change in beta band
365 amplitude for the set-size contrast (Figure 5B). Thus, the modulation of beta amplitude by set-
366 size was most likely driven by a difference in response time, whereas the modulation of beta
367 amplitude as a function of task abstraction is more likely driven by stimulus processing. No
368 significant delta band amplitude was observed time-locked to the period just prior to the
369 response. For the set-size contrast (Figure 5B), there was a significant increase in amplitude in
370 the theta frequency band (3-8 Hz), starting at 1500 milliseconds prior to a response and
371 persisted after the response. Thus, the significant change in theta amplitude as a function of
372 set-size most likely does not only reflect post-response processes, but also related to pre-
373 response stimulus processing.

374

375 *Relationship between neuronal oscillations and behavior*

376 Next, we investigated whether the significant changes in spectral amplitude during
377 different task conditions correlated with behavior. To test this, we extracted spectral amplitude
378 values from the significant time-frequency clusters for the abstraction (2-3 Hz delta and 18-22
379 Hz beta; Figure 3A) and set-size (4-6 Hz theta and 18-22 Hz beta; Figure 3B) contrasts from the
380 frontal midline electrode cluster, since this cluster showed the strongest peak in these contrasts
381 (Figure 3C-F). We correlated the change in beta and delta amplitude with the change in RT as a
382 function of abstraction. RT was analyzed since accuracy was at ceiling for many participants.
383 For the abstraction contrast, task differences in beta band amplitude was significantly negatively
384 correlated with RT ($r(30) = -0.59$, $p = 0.001$) and task differences in delta band amplitude was
385 significantly positively correlated with RT ($r(30) = 0.45$, $p = 0.012$; Figure 6A). For the set-size
386 contrast, we correlated the change in beta and theta amplitude with the change in RT as a
387 function of task set-size. We found that the increase in theta band amplitude was significantly
388 positively correlated with RT ($r(30) = 0.36$, $p = 0.047$), whereas there was no significant
389 relationship between beta band amplitude and behavior ($r(30) = -0.24$, $p = 0.20$; Figure 6B). Our
390 time frequency results (Figure 3) found that peak beta amplitude decreased from 12-18 Hz by
391 abstraction and decreased from 12-22Hz by set-size. Therefore, we examined whether the
392 observed behavioral correlation was consistent for the high (18-22Hz) and low (12-18Hz) beta
393 bands. Just as with the high beta band, amplitude in the low beta band significantly negatively
394 correlated with abstraction ($r(30) = -0.47$, $p = 0.008$) but did not show a significant relationship
395 with set-size ($r(30) = -0.15$, $p = 0.41$). Thus, we do not find evidence that low and high beta
396 serve different functional roles. Altogether, increased delta and decreased beta amplitude
397 correlated with increased response time as a function of rule abstraction, and increased theta
398 amplitude correlated with increased response time as a function of task set-size.

399

400 *Phase Amplitude Coupling Results*

401 Our results thus far provide evidence that delta and beta oscillations may reflect the
402 cognitive processes related to increased abstraction, whereas theta may reflect the cognitive
403 processes related to increased set-size. To further probe the interactions between these
404 oscillations in different frequency bands, we conducted a phase amplitude coupling (PAC)
405 analysis. We investigated the coupling strength of the phase of the slower frequency bands,
406 delta and theta, with the amplitude of the higher frequency bands, beta and gamma. The
407 comodulograms for each condition were calculated for the phase of low frequencies (2-7 Hz) to
408 the amplitude of high frequencies (10-49 Hz) (Figure 7). Since both delta and beta amplitude
409 were modulated as a function of the abstraction of the task condition, we focused our statistical
410 analysis on the coupling between delta phase (2-3 Hz) coupled to beta amplitude (18-22 Hz).
411 Given that we found theta-gamma PAC in our previous electrocorticography study with a similar
412 task (Voytek, Kayser et al. 2015), we also analyzed coupling of the phase of the theta frequency
413 band (4-6 Hz) with the amplitude of the gamma frequency band (40-49 Hz). We found a
414 significant increase in delta-beta PAC with increased abstraction ($F(1,30) = 7.62$, $p = 0.00976$,
415 $\eta^2_p = 0.203$; Figure 7A,B), but not set-size ($F(1,30) = 2.63$, $p = 0.115$, $\eta^2_p = 0.0807$), and there
416 was no interaction ($F(1,30) = 2.79$, $p = 0.105$, $\eta^2_p = 0.0852$). For theta-gamma PAC, we found a
417 significant increase in PAC for the low abstraction conditions relative to the high abstraction
418 conditions ($F(1,30) = 4.56$, $p = 0.0409$, $\eta^2_p = 0.132$; Figure 7C,D), but no effect of theta-gamma
419 PAC for set-size ($F(1,30) = 1.16$, $p = 0.290$, $\eta^2_p = 0.0372$), and no interaction ($F(1,30) = 0.591$, p
420 $= 0.448$, $\eta^2_p = 0.0193$). During the high abstraction, high set-size condition, we found a
421 significant increase in delta-beta PAC ($t(30) = 2.377$, $p = 0.012$, $d = 0.427$), one-tailed; Figure
422 7B) and beta amplitude was strongest at the trough and rise of delta phase (Figure 8A). During
423 the low abstraction, high set-size condition, we found a moderate increase in theta-gamma PAC
424 ($t(30) = 1.665$, $p = 0.053$, $d = 0.299$, one-tailed; Figure 7D) and gamma amplitude was strongest
425 at the rise of theta phase (Figure 8B). Therefore, delta-beta coupling may be how low frequency

426 oscillations modulate high frequency oscillations to execute abstract rules, whereas theta-
427 gamma coupling may be relevant for maintaining task rules with higher set size.

428

429 **Discussion**

430

431 In this experiment, we investigated the oscillatory neural dynamics associated with two
432 dissociable components of hierarchical cognitive control: rule abstraction and set-size. Previous
433 studies found that various frequency bands from low frequency delta to high frequency gamma
434 are associated with cognitive control (Helfrich and Knight 2016), but the specific contribution of
435 each of these bands to different control processes remains underspecified. We found that the
436 abstraction and set-size of task rules are each associated with distinct oscillatory mechanisms.
437 Specifically, when the abstractness of the rule increased, delta amplitude increased and beta
438 amplitude decreased; whereas when the number of rules (set-size) increased, theta amplitude
439 increased and beta amplitude decreased. These task-dependent changes in oscillatory
440 amplitude correlated with behavioral performance. When the abstraction of the rule increased,
441 slower response times correlated with increased delta amplitude and decreased beta amplitude.
442 When the set-size increased, slower response times correlated with increased theta amplitude.
443 Prior to the motor response, increased abstraction decreased beta amplitude, and increased
444 set-size increased theta amplitude. Finally, coupling between the phase of delta oscillations and
445 the amplitude of beta oscillations strengthened as a function of task abstraction.

446 Cognitive control is organized hierarchically such that superordinate abstract
447 representations influence subordinate, concrete action representations. In our previous study
448 using electrocorticography with a similar version of the task (Voytek, Kayser et al. 2015), we
449 found that tasks that engaged more abstract task rules increased theta synchrony between the
450 prefrontal cortex (PFC) and premotor cortex. Furthermore, we found theta phase in the PFC
451 coupled with gamma amplitude in premotor regions, suggesting that the PFC communicates

452 with the motor cortex for hierarchical control via theta-gamma phase amplitude coupling
453 (Voytek, Kayser et al. 2015). However, one important limitation of this previous study is that
454 tasks that required more abstract rules also had increased set-size; therefore, we could not
455 discern whether changes in oscillatory activities were driven by differences in abstraction or set-
456 size. An important feature of our current experiment was to separately manipulate the
457 abstraction of the rule and the number of competing rules (set-size). We further matched the
458 performance (accuracy) between high and low abstraction. Therefore, we were able to
459 dissociate these two components of hierarchical cognitive control.

460 Our findings suggest a relationship between theta oscillations and set-size, and this
461 finding is consistent with previous studies that reported theta oscillations scale with working
462 memory load (Jensen and Tesche 2002, Meltzer, Negishi et al. 2007, So, Wong et al. 2017,
463 Berger, Griesmayr et al. 2019). Other studies have also found that theta oscillations
464 (presumably from frontal cortex) increase during tasks that required cognitive control (Cohen
465 2011, Hsieh, Ekstrom et al. 2011, Kikumoto and Mayr 2018). Theta-gamma coupling has been
466 suggested as a mechanism by which multiple representations are organized for working
467 memory (Bahramisharif, Jensen et al. 2018) and long-term memory (Heusser, Poeppel et al.
468 2016). Therefore, the increased theta-gamma PAC for higher set-size in our task could reflect
469 the maintenance or retrieval of an increased number of rules. It should be noted that in our
470 previous study using electrocorticography, we found increased theta phase to high gamma
471 amplitude coupling for the high abstraction, high set-size condition (Voytek, Kayser et al. 2015).
472 While we were unable to measure theta to high gamma coupling due to the limitations of EEG,
473 we did find increased theta amplitude for this condition consistent with these findings.
474 Furthermore, this previous study did not separately manipulate abstraction and set-size, which
475 we investigated in the current study (see Methods).

476 We observed that beta amplitude decreased after stimulus onset as a function of
477 increased abstraction and increased set-size. For the response-locked analysis, beta

478 oscillations decreased only as a function of increased abstraction, but not increased set-size.
479 Many studies have found that beta oscillations decrease when the motor system executes an
480 action (Little and Brown 2012). While we also observed that beta band amplitude decreased
481 before the button press, higher abstraction conditions showed a greater beta amplitude
482 decrease when compared to lower abstraction conditions. We also found decreased beta
483 amplitude as a function of abstraction in the stimulus-locked analysis. Together, these
484 abstraction dependent results indicate a role for beta oscillations beyond motor preparation. We
485 propose that beta oscillations may reflect top-down inhibitory signals for guiding action that are
486 most robustly disengaged when guided by hierarchical goal representations.

487 Our findings of increased delta and decreased beta oscillations with increased
488 abstraction are consistent with a previous study that examined performance of a delayed-
489 match-to-sample task in which monkeys had to evaluate an object according to two different
490 categorical judgements: left versus right or up versus down (Antzoulatos and Miller 2016). This
491 study reported that distinct neural populations carry information for each of these two
492 categories: vertically selective populations and horizontally selective populations. For the cued
493 category, beta coherence increased between the neural populations that coded for the relevant
494 category. This pattern of activity led the authors to conclude that beta oscillations were encoding
495 rule categories. Our task also required the maintenance of abstract rules and similarly found an
496 abstraction-related modulation of beta amplitude in prefrontal cortex. Furthermore, when there
497 was a shift in the boundary between what was defined as “up” and “down,” there was an
498 increase in delta synchrony between prefrontal and parietal cortex. This suggests that updates
499 to abstract categorical rules modulates delta oscillations. In our experiment, for the high
500 abstraction, high set-size condition, participants had to evaluate the similarity of two different
501 objects based on different stimuli attributes (e.g., judge the similarity in texture or shape), and
502 the relevant attribute that participants should focus on was instructed by a supraordinate task
503 rule cued by the color of the square surrounding the stimuli. Based on the findings from

504 Antzoulatos & Miller 2016, the increase in delta oscillations in our study may reflect an update to
505 the relevant supraordinate rule, and the change in beta oscillations may reflect rule selection.

506 Participants with the greatest increase in response time when responding to the
507 increased abstraction conditions showed the greatest increase in delta amplitude and decrease
508 in beta amplitude. Similarly, participants with the greatest increase in response time when
509 responding to the increased set-size conditions showed the greatest increase in theta
510 amplitude. These findings emphasize the behavioral relevance of these low frequency neuronal
511 oscillations and provide further support for a role of delta oscillations in processing task
512 abstraction and theta oscillations in processing increased set-size.

513 The interplay between slow and fast neuronal oscillations has been investigated as a
514 mechanism for cognitive control (Sauseng, Klimesch et al. 2009, Sauseng, Griesmayr et al.
515 2010, Roux, Wibral et al. 2012, Voytek, Kayser et al. 2015) as long-range, low frequency
516 cognitive control signals from prefrontal cortex couple to more local high frequency oscillations
517 (Canolty and Knight 2010, Sauseng, Griesmayr et al. 2010). Our PAC analysis revealed that
518 delta phase coupled with beta amplitude when task conditions became more abstract.
519 Specifically, delta-beta coupling increased in the high abstraction, high set-size condition in
520 which participants decide between two task rules (e.g., focus on texture or shape). We observed
521 that beta amplitude decreased around the peak of the delta phase (see Figure 8A). This finding
522 is similar to Helfrich et al. (2017) in which alpha-beta amplitude was lowest at peak delta-phase
523 in prefrontal cortex during a perceptual judgement (Helfrich, Huang et al. 2017). Wyart et al.
524 (2012) also reported that the distribution of beta oscillations in motor cortex was updated every
525 cycle of a prefrontal delta signal, and the amplitude of beta was inversely related to the
526 probability of action of the underlying motor cortex (Wyart, de Gardelle et al. 2012). Consistent
527 with Wyart et al. 2012, our PAC finding suggests that delta phase in frontal regions may guide
528 action selection via modulating beta-band amplitude when cognitive tasks are hierarchically

529 organized, and participants have to rely on supraordinate, abstract rules to guide concrete
530 actions.

531 Taken together, low frequency oscillations in the theta and delta frequency band may
532 reflect different components of hierarchical cognitive control that couple to different high
533 frequency oscillations. Gamma oscillations play a primary role in carrying feedforward sensory
534 processing signals (Börgers and Kopell 2008, Michalareas, Vezoli et al. 2016). Theta
535 oscillations in prefrontal cortex couple with gamma oscillations to support the organization of
536 perceptual information during memory encoding and retrieval (Osipova, Takashima et al. 2006,
537 Hsieh and Ranganath 2014). When multiple items must be held in mind, theta-gamma coupling
538 is increased (Alekseichuk, Turi et al. 2016, Tamura, Spellman et al. 2017, Bahramisharif,
539 Jensen et al. 2018). Our findings suggest that increasing the set-size of a task may recruit a
540 similar neural mechanism. Beta oscillations play a role in sensory feedback (Bastos, Vezoli et
541 al. 2015, Michalareas, Vezoli et al. 2016) and motor control (Zhang, Chen et al. 2008, Picazio,
542 Veniero et al. 2014). Therefore, delta to beta coupling may be a mechanism by which low
543 frequency oscillations in prefrontal cortex guide future action according to abstract goals.
544 Theoretical models on the role of gamma and beta oscillations in bottom-up and top-down
545 attention (Fries 2015, Riddle, Hwang et al. 2019) may be extended to include theta and delta
546 oscillations that show task-related modulations in the frontal cortex.

547

548 **References**

- 549 Alekseichuk, I., Z. Turi, G. A. de Lara, A. Antal and W. Paulus (2016). "Spatial working memory
550 in humans depends on theta and high gamma synchronization in the prefrontal cortex."
551 *Current Biology* **26**(12): 1513-1521.
- 552 Antzoulatos, E. G. and E. K. Miller (2014). "Increases in functional connectivity between
553 prefrontal cortex and striatum during category learning." *Neuron* **83**(1): 216-225.

- 554 Antzoulatos, E. G. and E. K. Miller (2016). "Synchronous beta rhythms of frontoparietal
555 networks support only behaviorally relevant representations." Elife **5**: e17822.
- 556 Arnal, L. H., K. B. Doelling and D. Poeppel (2014). "Delta–beta coupled oscillations underlie
557 temporal prediction accuracy." Cerebral Cortex **25**(9): 3077-3085.
- 558 Badre, D. and M. D'Esposito (2007). "Functional magnetic resonance imaging evidence for a
559 hierarchical organization of the prefrontal cortex." Journal of cognitive neuroscience
560 **19**(12): 2082-2099.
- 561 Badre, D. and M. D'Esposito (2009). "Is the rostro-caudal axis of the frontal lobe hierarchical?"
562 Nature Reviews Neuroscience **10**(9): 659.
- 563 Badre, D. and D. E. Nee (2018). "Frontal cortex and the hierarchical control of behavior." Trends
564 in cognitive sciences **22**(2): 170-188.
- 565 Bahramisharif, A., O. Jensen, J. Jacobs and J. Lisman (2018). "Serial representation of items
566 during working memory maintenance at letter-selective cortical sites." PLoS biology
567 **16**(8): e2003805.
- 568 Bastos, A. M., J. Vezoli, C. A. Bosman, J.-M. Schoffelen, R. Oostenveld, J. R. Dowdall, P. De
569 Weerd, H. Kennedy and P. Fries (2015). "Visual areas exert feedforward and feedback
570 influences through distinct frequency channels." Neuron **85**(2): 390-401.
- 571 Berger, B., B. Griesmayr, T. Minarik, A. Biel, D. Pinal, A. Sterr and P. Sauseng (2019).
572 "Dynamic regulation of interregional cortical communication by slow brain oscillations
573 during working memory." Nature communications **10**.
- 574 Blair, R. C. and W. Karniski (1993). "An alternative method for significance testing of waveform
575 difference potentials." Psychophysiology **30**(5): 518-524.
- 576 Börgers, C. and N. J. Kopell (2008). "Gamma oscillations and stimulus selection." Neural
577 computation **20**(2): 383-414.
- 578 Braver, T. S. (2012). "The variable nature of cognitive control: a dual mechanisms framework."
579 Trends in cognitive sciences **16**(2): 106-113.

- 580 Buschman, T. J., E. L. Denovellis, C. Diogo, D. Bullock and E. K. Miller (2012). "Synchronous
581 oscillatory neural ensembles for rules in the prefrontal cortex." Neuron **76**(4): 838-846.
- 582 Canolty, R. T. and R. T. Knight (2010). "The functional role of cross-frequency coupling." Trends
583 in cognitive sciences **14**(11): 506-515.
- 584 Cavanagh, J. F. and M. J. Frank (2014). "Frontal theta as a mechanism for cognitive control."
585 Trends in cognitive sciences **18**(8): 414-421.
- 586 Clarke, A., B. M. Roberts and C. Ranganath (2018). "Neural oscillations during conditional
587 associative learning." NeuroImage **174**: 485-493.
- 588 Cohen, M. X. (2011). "Hippocampal-prefrontal connectivity predicts midfrontal oscillations and
589 long-term memory performance." Current Biology **21**(22): 1900-1905.
- 590 Cohen, M. X. (2014). Analyzing neural time series data: theory and practice, MIT press.
- 591 Cohen, M. X. (2019). "A better way to define and describe Morlet wavelets for time-frequency
592 analysis." NeuroImage **199**: 81-86.
- 593 Delorme, A. and S. Makeig (2004). "EEGLAB: an open source toolbox for analysis of single-trial
594 EEG dynamics including independent component analysis." Journal of neuroscience
595 methods **134**(1): 9-21.
- 596 Fell, J. and N. Axmacher (2011). "The role of phase synchronization in memory processes."
597 Nature reviews neuroscience **12**(2): 105.
- 598 Fries, P. (2015). "Rhythms for cognition: communication through coherence." Neuron **88**(1):
599 220-235.
- 600 Gruber, M. J., A. J. Watrous, A. D. Ekstrom, C. Ranganath and L. J. Otten (2013). "Expected
601 reward modulates encoding-related theta activity before an event." Neuroimage **64**: 68-
602 74.
- 603 Helfrich, R. F., A. Breska and R. T. Knight (2019). "Neural entrainment and network resonance
604 in support of top-down guided attention." Current opinion in psychology.

- 605 Helfrich, R. F., M. Huang, G. Wilson and R. T. Knight (2017). "Prefrontal cortex modulates
606 posterior alpha oscillations during top-down guided visual perception." Proceedings of
607 the National Academy of Sciences **114**(35): 9457-9462.
- 608 Helfrich, R. F. and R. T. Knight (2016). "Oscillatory dynamics of prefrontal cognitive control."
609 Trends in cognitive sciences **20**(12): 916-930.
- 610 Heusser, A. C., D. Poeppel, Y. Ezzyat and L. Davachi (2016). "Episodic sequence memory is
611 supported by a theta-gamma phase code." Nature neuroscience **19**(10): 1374.
- 612 Hsieh, L.-T., A. D. Ekstrom and C. Ranganath (2011). "Neural oscillations associated with item
613 and temporal order maintenance in working memory." Journal of Neuroscience **31**(30):
614 10803-10810.
- 615 Hsieh, L.-T. and C. Ranganath (2014). "Frontal midline theta oscillations during working memory
616 maintenance and episodic encoding and retrieval." Neuroimage **85**: 721-729.
- 617 Jensen, O. and C. D. Tesche (2002). "Frontal theta activity in humans increases with memory
618 load in a working memory task." European journal of Neuroscience **15**(8): 1395-1399.
- 619 Kikumoto, A. and U. Mayr (2018). "Decoding hierarchical control of sequential behavior in
620 oscillatory EEG activity." eLife **7**: e38550.
- 621 Lisman, J. E. and O. Jensen (2013). "The theta-gamma neural code." Neuron **77**(6): 1002-1016.
- 622 Little, S. and P. Brown (2012). "What brain signals are suitable for feedback control of deep
623 brain stimulation in Parkinson's disease?" Annals of the New York Academy of Sciences
624 **1265**(1): 9-24.
- 625 Maris, E. and R. Oostenveld (2007). "Nonparametric statistical testing of EEG-and MEG-data."
626 Journal of neuroscience methods **164**(1): 177-190.
- 627 Meltzer, J. A., M. Negishi, L. C. Mayes and R. T. Constable (2007). "Individual differences in
628 EEG theta and alpha dynamics during working memory correlate with fMRI responses
629 across subjects." Clinical Neurophysiology **118**(11): 2419-2436.

- 630 Michalareas, G., J. Vezoli, S. Van Pelt, J.-M. Schoffelen, H. Kennedy and P. Fries (2016).
631 "Alpha-beta and gamma rhythms subserve feedback and feedforward influences among
632 human visual cortical areas." Neuron **89**(2): 384-397.
- 633 Miller, B. T. and M. D'Esposito (2005). "Searching for "the top" in top-down control." Neuron
634 **48**(4): 535-538.
- 635 Miller, E. K. and J. D. Cohen (2001). "An integrative theory of prefrontal cortex function." Annual
636 review of neuroscience **24**(1): 167-202.
- 637 Morillas-Romero, A., M. Tortella-Feliu, X. Bornas and P. Putman (2015). "Spontaneous EEG
638 theta/beta ratio and delta-beta coupling in relation to attentional network functioning and
639 self-reported attentional control." Cognitive, Affective, & Behavioral Neuroscience **15**(3):
640 598-606.
- 641 Nácher, V., A. Ledberg, G. Deco and R. Romo (2013). "Coherent delta-band oscillations
642 between cortical areas correlate with decision making." Proceedings of the National
643 Academy of Sciences **110**(37): 15085-15090.
- 644 Norman, D. A. and T. Shallice (1986). Attention to action. Consciousness and self-regulation,
645 Springer: 1-18.
- 646 Osipova, D., A. Takashima, R. Oostenveld, G. Fernández, E. Maris and O. Jensen (2006).
647 "Theta and gamma oscillations predict encoding and retrieval of declarative memory."
648 Journal of neuroscience **26**(28): 7523-7531.
- 649 Picazio, S., D. Veniero, V. Ponzio, C. Caltagirone, J. Gross, G. Thut and G. Koch (2014).
650 "Prefrontal control over motor cortex cycles at beta frequency during movement
651 inhibition." Current Biology **24**(24): 2940-2945.
- 652 Riddle, J., S. Ahn, T. McPherson, S. Girdler and F. Frohlich (2020). "Progesterone modulates
653 theta oscillations in the frontal-parietal network." bioRxiv: 2020.2001.2016.909374.

- 654 Riddle, J., K. Hwang, D. Cellier, S. Dhanani and M. D'Esposito (2019). "Causal Evidence for the
655 Role of Neuronal Oscillations in Top–Down and Bottom–Up Attention." Journal of
656 cognitive neuroscience **31**(5): 768-779.
- 657 Roux, F. and P. J. Uhlhaas (2014). "Working memory and neural oscillations: alpha–gamma
658 versus theta–gamma codes for distinct WM information?" Trends in cognitive sciences
659 **18**(1): 16-25.
- 660 Roux, F., M. Wibral, H. M. Mohr, W. Singer and P. J. Uhlhaas (2012). "Gamma-band activity in
661 human prefrontal cortex codes for the number of relevant items maintained in working
662 memory." Journal of Neuroscience **32**(36): 12411-12420.
- 663 Sadaghiani, S. and A. Kleinschmidt (2016). "Brain networks and α -oscillations: structural and
664 functional foundations of cognitive control." Trends in cognitive sciences **20**(11): 805-
665 817.
- 666 Sasaki, K., T. Tsujimoto, S. Nishikawa, N. Nishitani and T. Ishihara (1996). "Frontal mental theta
667 wave recorded simultaneously with magnetoencephalography and
668 electroencephalography." Neuroscience research **26**(1): 79-81.
- 669 Sauseng, P., B. Griesmayr, R. Freunberger and W. Klimesch (2010). "Control mechanisms in
670 working memory: a possible function of EEG theta oscillations." Neuroscience &
671 Biobehavioral Reviews **34**(7): 1015-1022.
- 672 Sauseng, P., W. Klimesch, K. F. Heise, W. R. Gruber, E. Holz, A. A. Karim, M. Glennon, C.
673 Gerloff, N. Birbaumer and F. C. Hummel (2009). "Brain oscillatory substrates of visual
674 short-term memory capacity." Current biology **19**(21): 1846-1852.
- 675 So, W. K., S. W. Wong, J. N. Mak and R. H. Chan (2017). "An evaluation of mental workload
676 with frontal EEG." PloS one **12**(4): e0174949.
- 677 Stropahl, M., A.-K. R. Bauer, S. Debener and M. G. Bleichner (2018). "Source-modelling
678 auditory processes of EEG data using EEGLAB and Brainstorm." Frontiers in
679 neuroscience **12**: 309.

- 680 Tamura, M., T. J. Spellman, A. M. Rosen, J. A. Gogos and J. A. Gordon (2017). "Hippocampal-
681 prefrontal theta-gamma coupling during performance of a spatial working memory task."
682 Nature communications **8**(1): 1-9.
- 683 Todd, M. T., L. E. Nystrom and J. D. Cohen (2013). "Confounds in multivariate pattern analysis:
684 theory and rule representation case study." Neuroimage **77**: 157-165.
- 685 Vogelsang, D. A. and M. D'Esposito (2018). "Is there evidence for a rostral-caudal gradient in
686 fronto-striatal loops and what role does dopamine play?" Frontiers in neuroscience **12**:
687 242.
- 688 Vogelsang, D. A., M. Gruber, Z. M. Bergström, C. Ranganath and J. S. Simons (2018). "Alpha
689 oscillations during incidental encoding predict subsequent memory for new "foil"
690 information." Journal of cognitive neuroscience **30**(5): 667-679.
- 691 Voytek, B., A. S. Kayser, D. Badre, D. Fegen, E. F. Chang, N. E. Crone, J. Parvizi, R. T. Knight
692 and M. D'Esposito (2015). "Oscillatory dynamics coordinating human frontal networks in
693 support of goal maintenance." Nature neuroscience **18**(9): 1318.
- 694 Wutz, A., R. Loonis, J. E. Roy, J. A. Donoghue and E. K. Miller (2018). "Different levels of
695 category abstraction by different dynamics in different prefrontal areas." Neuron **97**(3):
696 716-726. e718.
- 697 Wyart, V., V. de Gardelle, J. Scholl and C. Summerfield (2012). "Rhythmic fluctuations in
698 evidence accumulation during decision making in the human brain." Neuron **76**(4): 847-
699 858.
- 700 Zhang, Y., Y. Chen, S. L. Bressler and M. Ding (2008). "Response preparation and inhibition:
701 the role of the cortical sensorimotor beta rhythm." Neuroscience **156**(1): 238-246.

702

703 Figure 1. Hierarchical cognitive control task

704 (A) The hierarchical cognitive control task used a two by two design with four conditions. On the
705 X-axis, the set-size increases within a fixed level of abstraction. On the Y-axis, the level of

706 abstraction increases. Behavioral results for response time (B) and accuracy (C). Error bars are
707 S.E.M.

708

709 **Figure 2. Electrode clusters used for EEG analysis**

710 Hierarchical clustering of the time-frequency data for each electrode revealed six distinct
711 electrode clusters. The analysis focused on the frontal midline electrode cluster
712 (outlined). The other electrode clusters were used for cluster-mass permutation testing in
713 time-frequency analysis.

714

715 **Figure 3. Time-frequency analysis of hierarchical cognitive control along two**
716 **dimensions: abstraction and set-size**

717 In the frontal-midline electrode cluster, there was a significant increase in delta and
718 decrease in beta amplitude as a function of task abstraction (A). The dark outline
719 highlights time-frequency clusters that were found to be significant at $p < 0.05$ and
720 survived correction for multiple comparisons. Delta amplitude increase was localized to
721 the frontal-midline and right frontal (B). Beta amplitude decrease was localized to the
722 frontal- and central-midline (C). In the frontal-midline electrode cluster, there was a
723 significant increase in theta amplitude and decrease in beta amplitude as a function of
724 task set-size. The increase in theta amplitude was localized to the frontal-midline
725 electrodes (E). The decrease in beta amplitude was localized to frontal-midline
726 electrodes (F).

727

728 **Figure 4. Time course of task-evoked oscillatory amplitude**

729 At time 0, the stimulus for the task is presented. (A) Delta amplitude showed the greatest
730 increase in the two high abstraction conditions (red and orange). (B) Theta amplitude
731 showed the greatest in the response task (dark blue and light blue) in the first 0.5

732 seconds and the greatest increase in the high set-size conditions (dark blue and red) in
733 the 1 to 2 second range. (C) Beta amplitude showed the greatest decrease in the high
734 abstraction, high set-size condition (red). Error bars are S.E.M.

735

736 **Figure 5. Response-locked time frequency analysis**

737 The response-locked time frequency analysis for the abstraction (A) and set-size (B)
738 contrast in the midfrontal electrode cluster found a significant decrease in low beta
739 amplitude prior to response for abstraction and increase in theta amplitude prior to and
740 after response for set-size. The line at time 0 is the time that the participant made a
741 response. The dark outline highlights time-frequency clusters that were found to be
742 significant at $p < 0.05$ with a cluster correction of $k = 100$.

743

744 **Figure 6. Behavior to brain correlations**

745 Correlation analysis for response time to spectral density for the significant clusters in
746 abstraction (A) and set-size (B). Error bars are 95% confidence intervals. * $p < 0.05$, ** p
747 < 0.005 , n.s. = not significant.

748

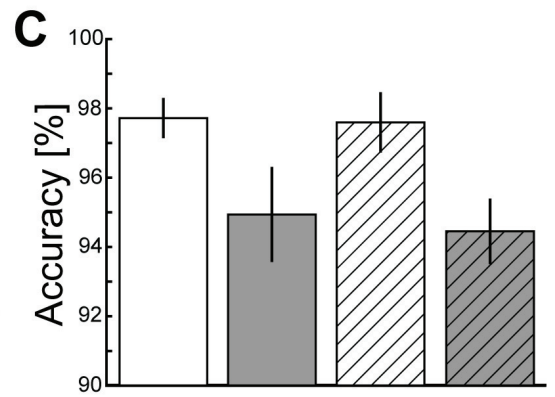
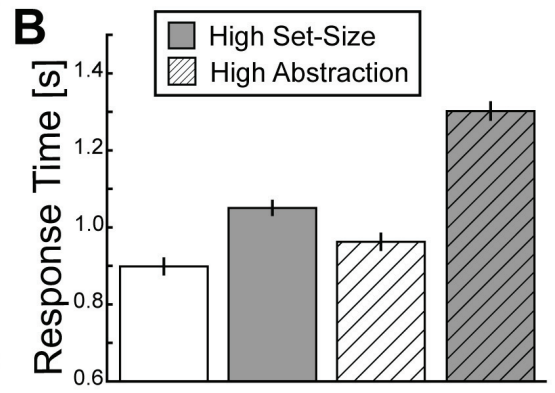
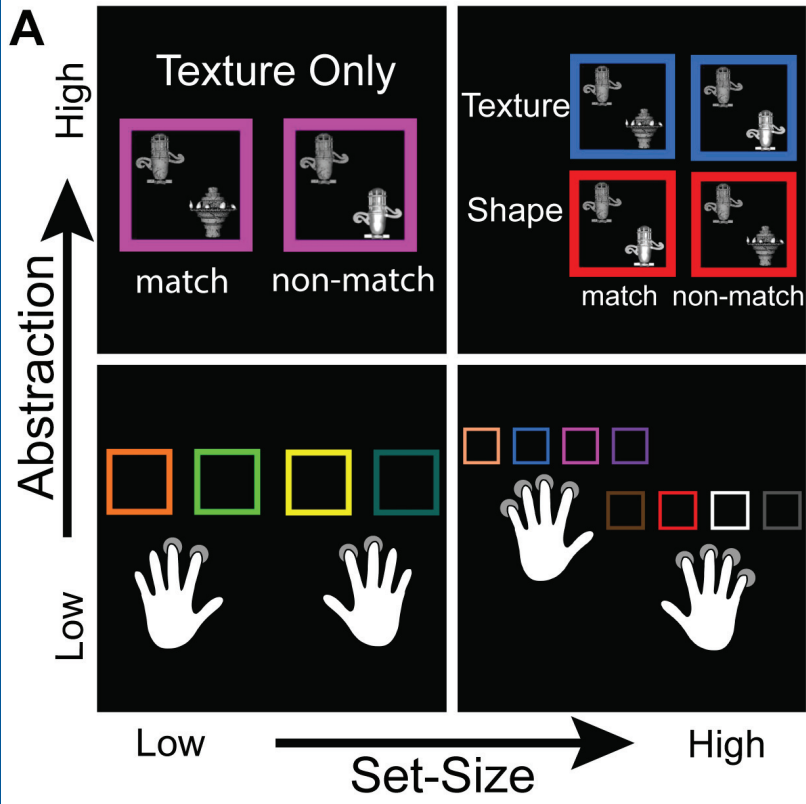
749 **Figure 7. Comodulograms of phase amplitude coupling for each task condition**

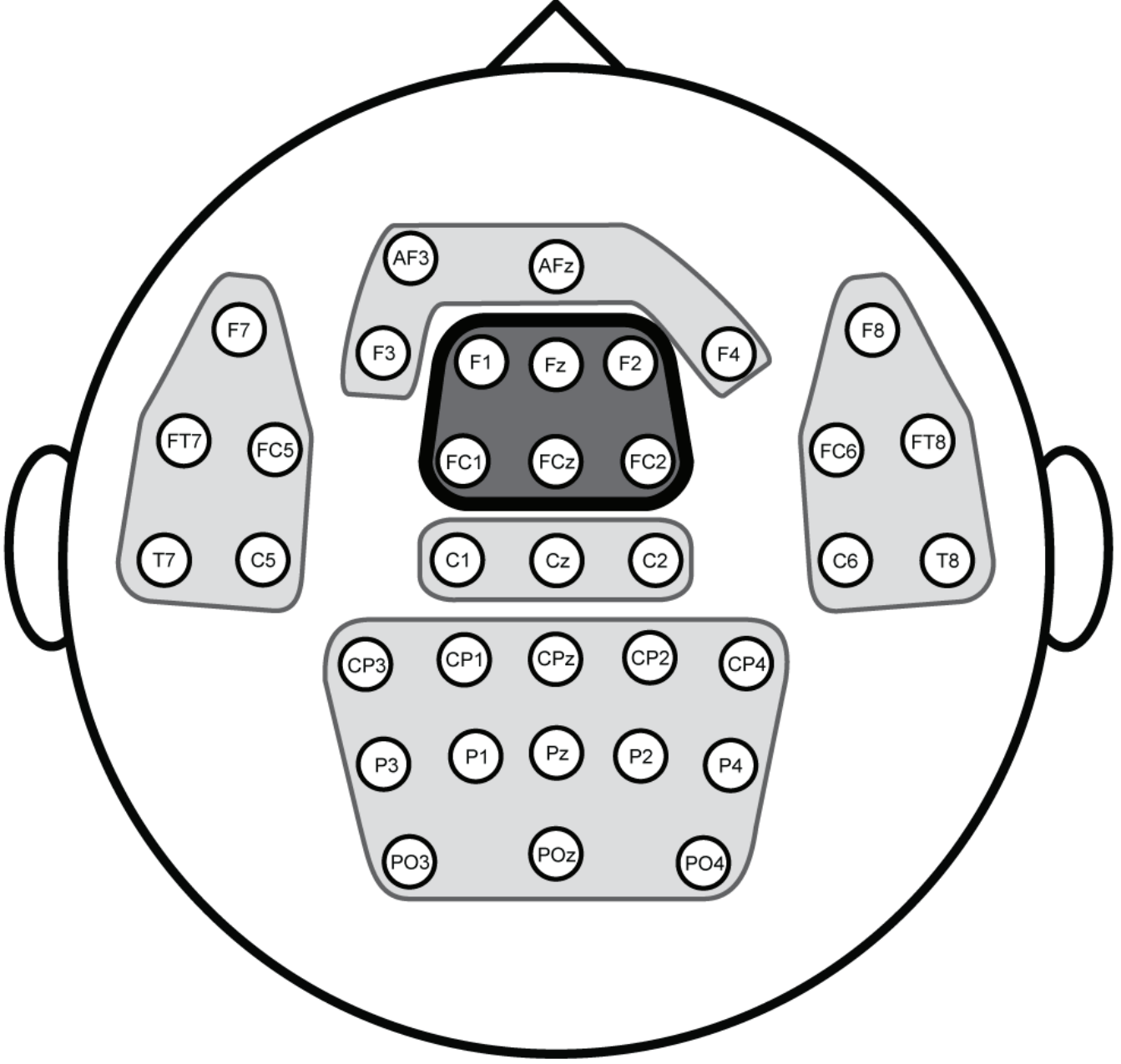
750 For the high abstraction conditions, there was increased coupling between delta phase
751 (2-3 Hz) and beta amplitude (18-22 Hz) in the high-set (B), but not low set-size condition
752 (A). For the low abstraction conditions, there was increased coupling between theta
753 phase (4-6 Hz) and gamma amplitude (40-49 Hz) in the low and high set-size conditions
754 (C, D).

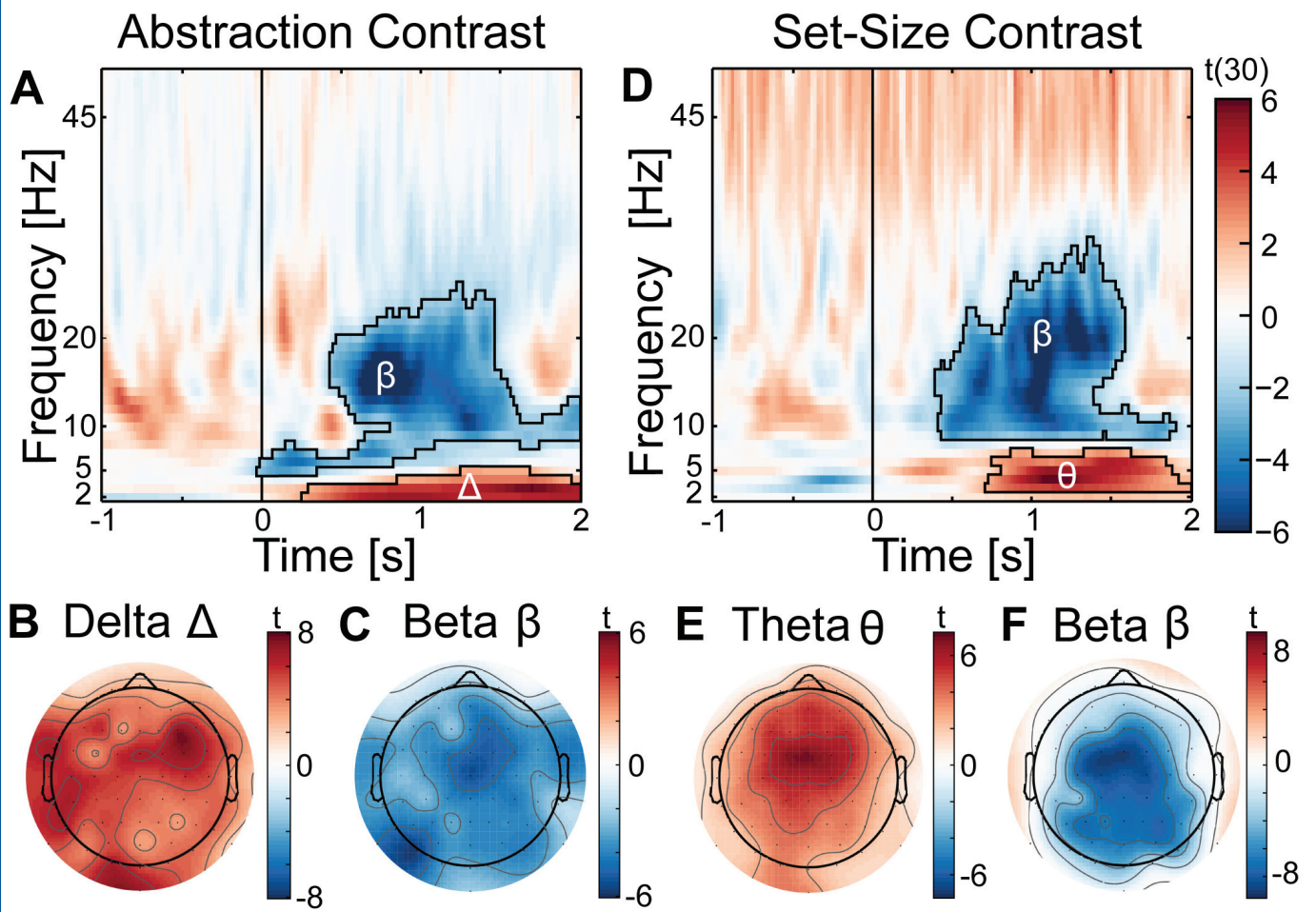
755

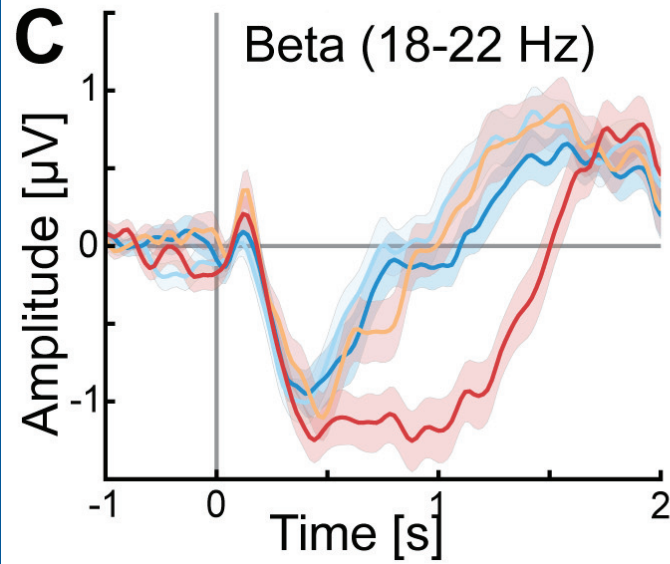
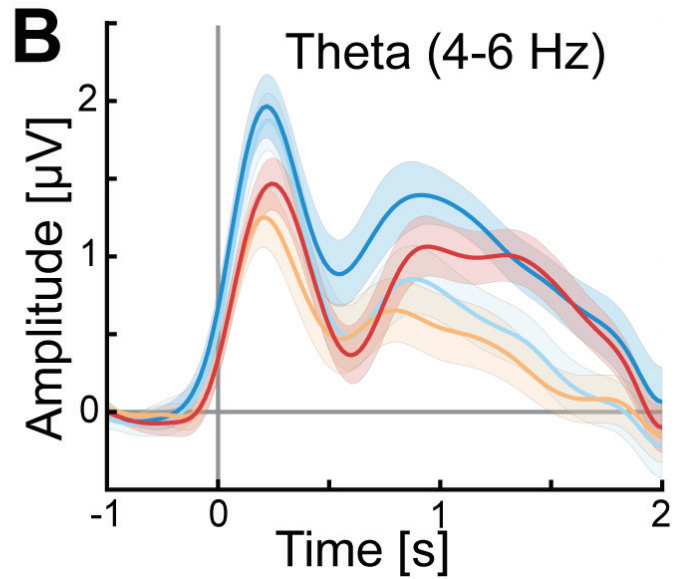
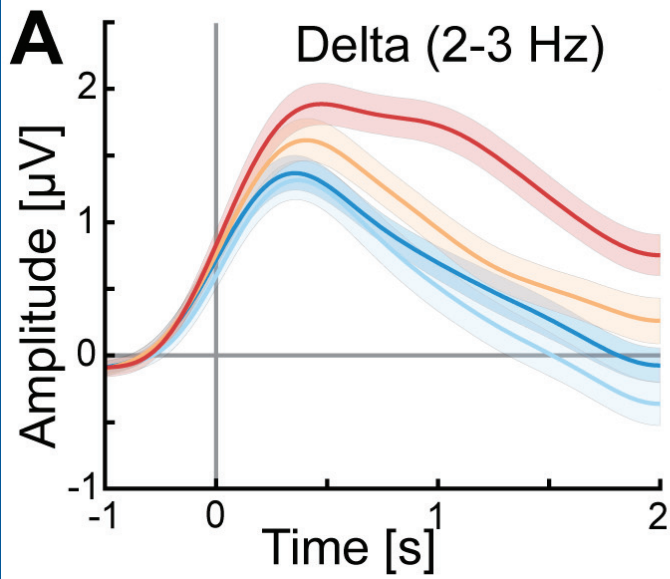
756 **Figure 8. Distribution of beta and gamma amplitude across delta and theta phase**

757 Rose plots of delta phase coupled to beta amplitude (A) for the high abstraction, high
758 set-size condition and theta phase coupled to gamma amplitude (B) for the low
759 abstraction, high set-size condition. Amplitude values (z) were binned into 30 phase
760 angles, averaged, and z-scored across phase bins. Error bars are within-participant
761 SEM. Legends depict the peak and trough values in radians.

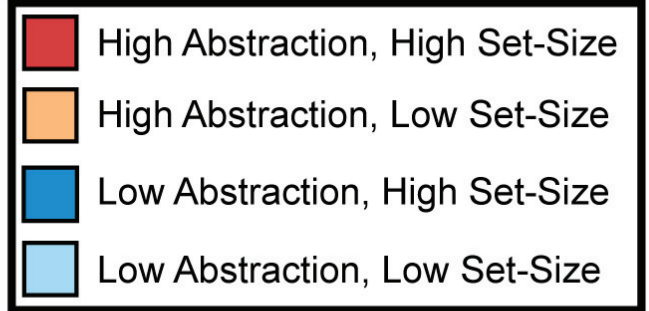




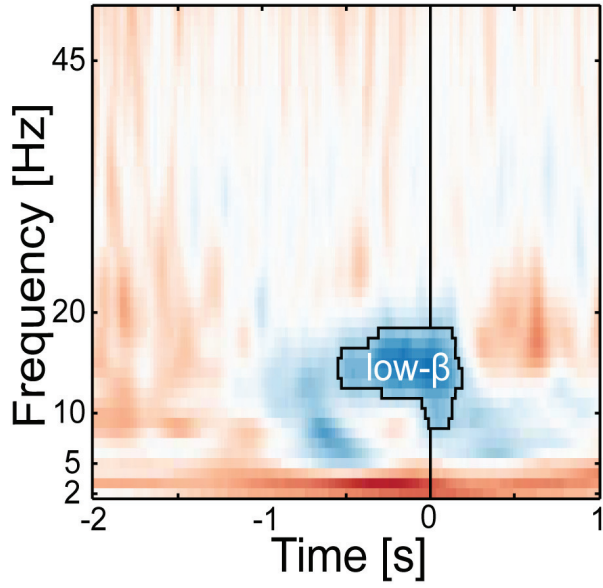




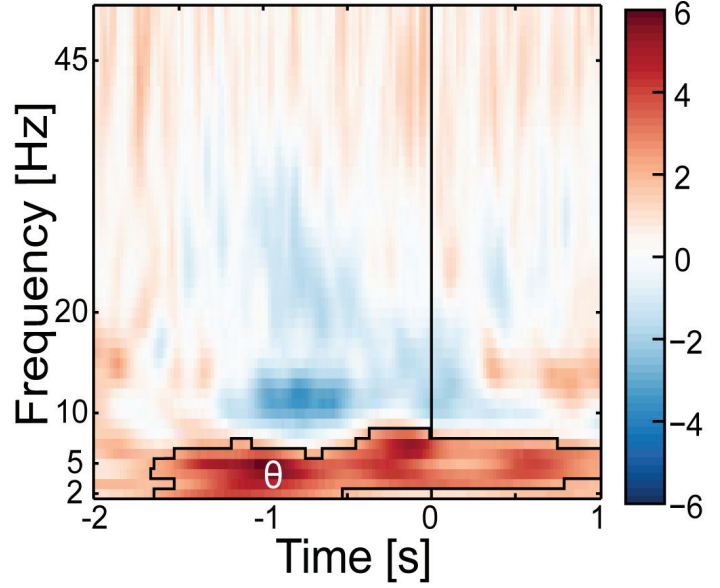
Task Condition

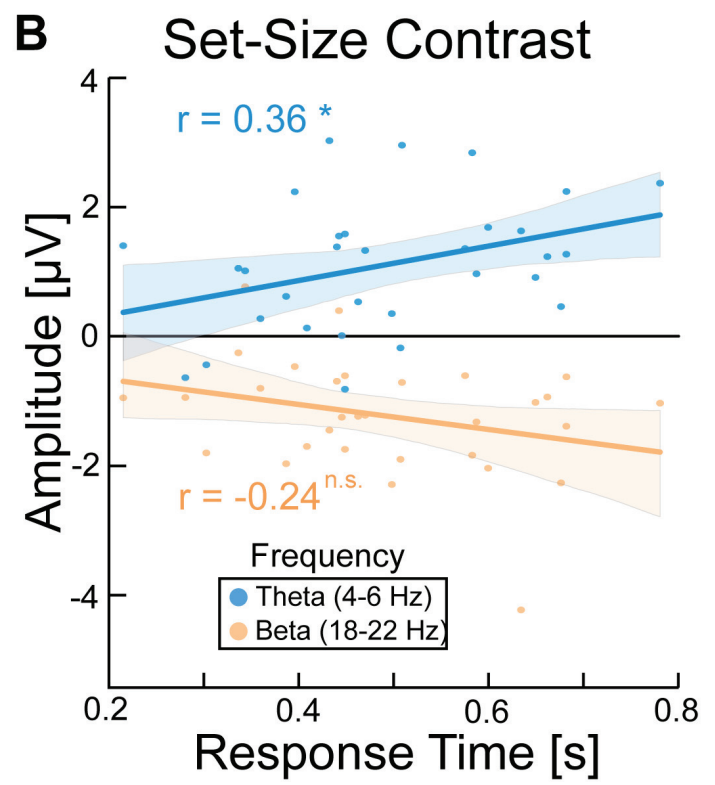
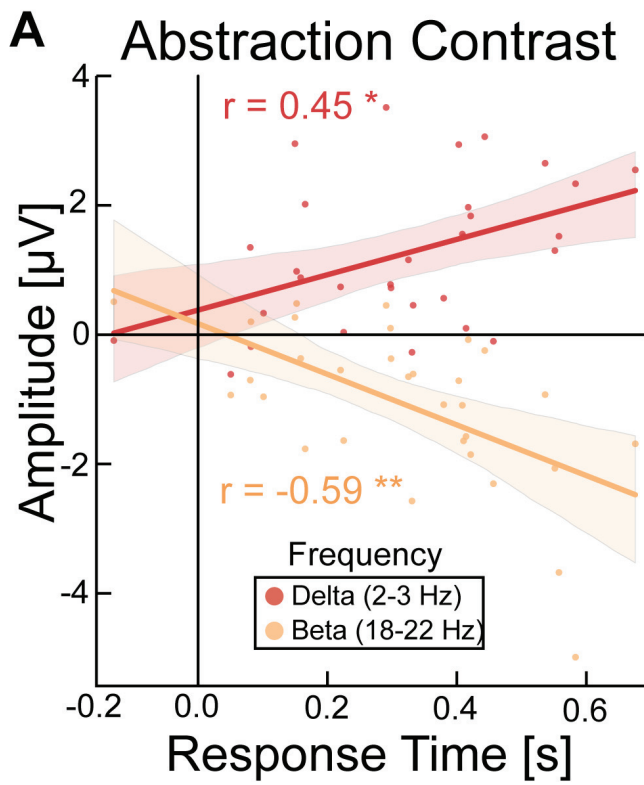


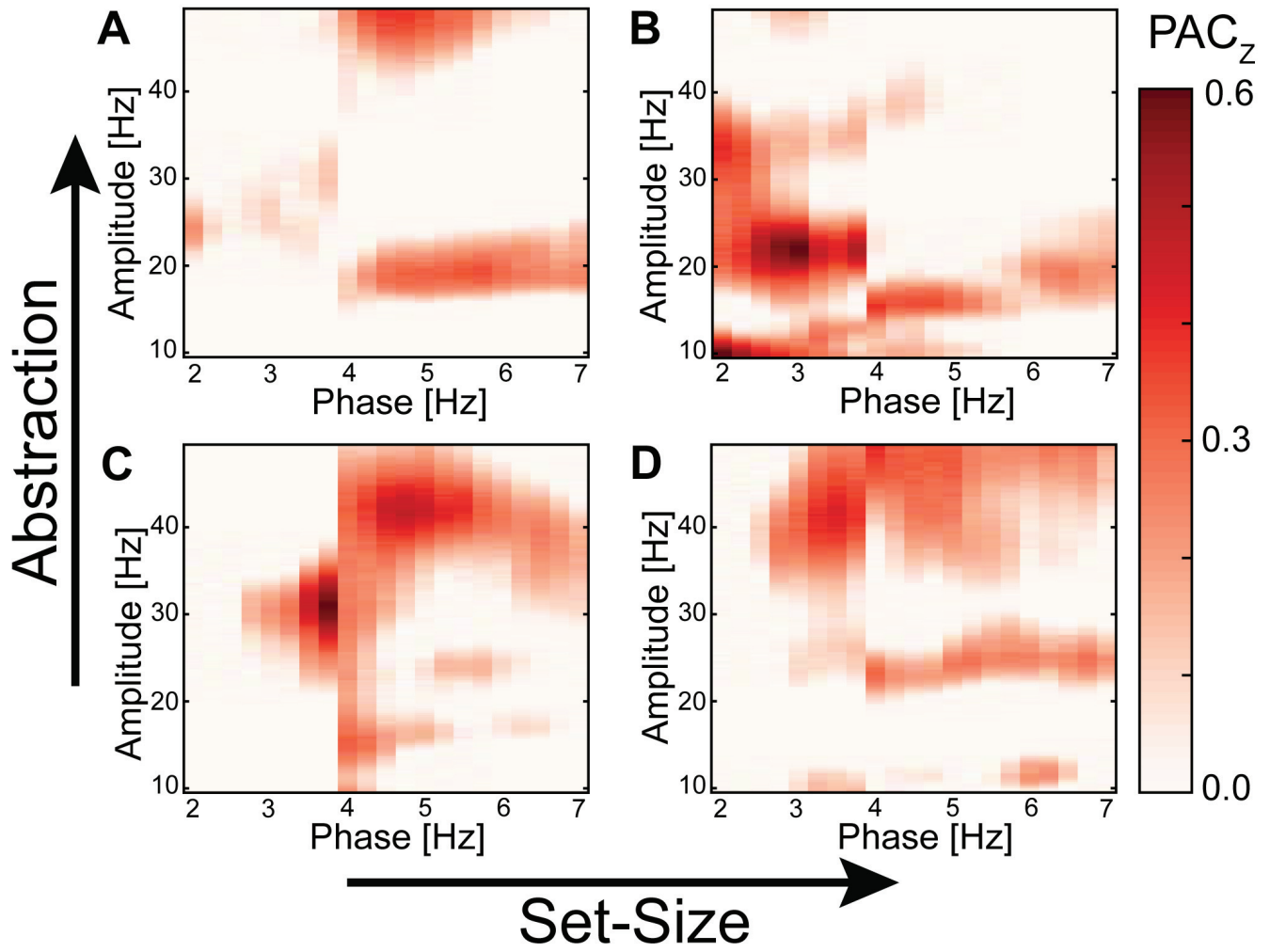
A Abstraction Contrast



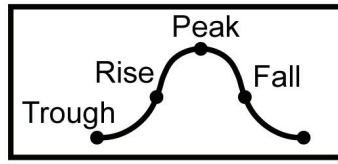
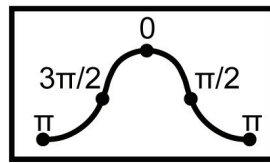
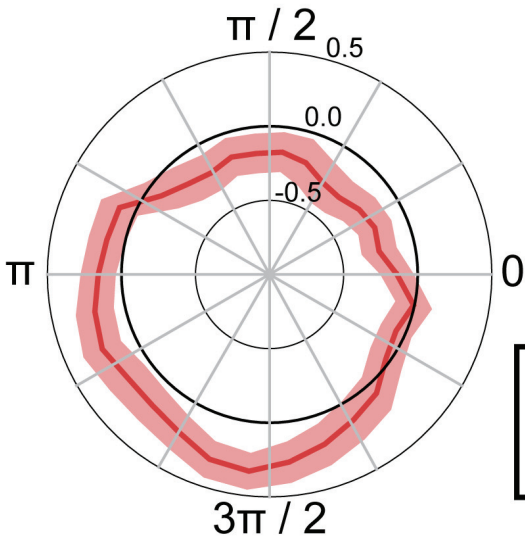
B Set-Size Contrast







A Delta-Beta (2-3, 18-22)



B Theta-Gamma (4-6, 40-49)

